Materials Horizons

Unveil Underlying Mechanism of Record-High Efficiency Organic Near-infrared Photodetector Harnessing Single-Component Photoactive Layer

Journal:	*Materials Horizons*
Manuscript ID	MH-COM-09-2019-001524.R2
Article Type:	Communication
Date Submitted by the Author:	23-Dec-2019

Complete List of Authors:	Wang, Miaosheng; University of Tennessee, Materials Science and Engineering Li, Ya-Ze; Ming Chi University of Technology Chen, Hung-Cheng; National Taiwan University Liu, Che-Wei; Ming Chi University of Technology Chen, Yi-Sheng; National Taiwan University Lo, Yuan-Chih ; National Taiwan University Tsao, Cheng-Si; Institute of Nuclear Energy Research, Huang, Yu-Ching; Institute of Nuclear Energy Research, Liu, Shun-Wei; Ming Chi University of Technology, Department of Electronic Engineering Wong, Ken-Tsung; National Taiwan University, Department of Chemistry Hu, Bin; University of Tennessee Knoxville

New concepts

In this work, for the first time, by utilizing the four-fold symmetric ClAlPc molecules as the *single-component active layer*, we have successfully demonstrated the record-high efficiency near infrared (NIR) thin-film organic photodetector (OPD) comparable with commercial standard silicon photodetector (Si-PD). The ClAlPc OPD shows the record-high external quantum efficiency (EQE) value of 43 % (at 3 V). Meanwhile, this ClAlPc OPD exhibits the largest linear dynamic range (LDR) of 170 dB with 8-order magnitude difference in photocurrent response as compared with ever reported NIR OPDs. With the ultra-thin (10nm) single component active layer design, the ClAlPc OPD can realize high response speed similar with Si-PD. The demonstration of this high efficiency *single-component active layer* OPD indicates the new fundamental mechanism to directly generate free photocarriers without using heterojunctions in organic materials. By using the magneto-photocurrent as an *in-situ* method to monitor the dissociation of photogenerated electron-hole pairs, we found that increasing the symmetry of charge density can significantly lower the electron-hole binding energy from eV to meV order. Clearly, increasing the symmetry of charge density through planar conjugated macrocyclic design presents a new mechanism to significantly lower the electron-hole binding energy in organic materials towards thin-film energy-related optoelectronic applications.

Unveil Underlying Mechanism of Record-High Efficiency Organic Near-infrared Photodetector Harnessing Single-Component Photoactive Layer

Miaosheng Wang[a], Ya-Ze Li[b], Hung-Cheng Chen[c], Che-Wei Liu[b], Yi-Sheng Chen[c], Yuan-Chih Lo[c], Cheng-Si Tsao[f,g], Yu-Ching Huang[h], Shun-Wei Liu[b,d,*], Ken-Tsung Wong[c,e,*], and Bin Hu[a,*]

[a] *Department of Materials Science and Engineering, University of Tennessee, Knoxville, TN 37996, USA*

[b] *Department of Electronic Engineering, Ming Chi University of Technology, New Taipei City 24301, Taiwan*

[c] *Department of Chemistry, National Taiwan University, Taipei 10617, Taiwan*

[d] *Organic Electronics Research Center, Ming Chi University of Technology, New Taipei City 24301, Taiwan*

[e] *Institute of Atomic and Molecular Science, Academia Sinica, Taipei 10617, Taiwan*

[f] *Deptartment of Materials Science and Engineering, National Taiwan University, Taipei 106, Taiwan.*

[g] *Institute of Nuclear Energy Research, Taoyuan 325, Taiwan*

[h] *Department of Materials Engineering, Ming Chi University of Technology, New Taipei City 24301, Taiwan*

*Corresponding authors:

Shun-Wei Liu: Email: swliu@mail.mcut.edu.tw

Ken-Tsung Wong: Email: kenwong@ntu.edu.tw

Bin Hu, E-mail: bhu@utk.edu

Abstract

This paper demonstrates high-efficiency organic near-infrared (NIR) photodetection activities by increasing the symmetry of photoinduced charge density based on planar cyclic donor-acceptor structures. The record-high photosensing capability (gain: $3x10^5$ and EQE: 43% at 3 V) is realized under the NIR 780 nm illumination upon using the single-component active layer chloroaluminum phthalocyanine (ClAlPc) with planar cyclic intramolecular donor-acceptor structures to create four-fold symmetry of photoinduced charge density. Our *in-situ* measurement of using bias-dependent magneto-photocurrent reveals that increasing the symmetry of photoinduced charge density through planar cyclic intramolecular donor-acceptor structures can significantly decrease the electron-hole binding energies, allowing the direct generation of free photogenerated carriers without any heterojunction structures. Particularly, with the four-fold symmetry of photoinduced charge density, the dissociation of electron-hole pairs can be completed at an extremely low critical bias (24.8 mV) in the ClAlPc molecules. Such low critical bias provides the underlying mechanisms to directly generate free carriers in single-component active layer under NIR illumination. Clearly, by using planar cyclic intramolecular donor-acceptor structures, symmetrically arranging photoinduced charge density presents a fundamental strategy to develop high-efficiency NIR sensing capabilities with single-component active layer design in organic molecules.

Introduction

Organic photodetectors (OPDs) converting light energy into electric current are aiming for the precise detection of low-level photons. The absorption features of organic materials allow OPDs performing wide spectral response together with low dark current density, high sensitivity, and reasonably fast response time, rendering this technology feasible for applications such as image sensor [1] and artificial vision [2]. Particularly interesting, near-infrared (NIR) responsive OPDs are emerging candidates for biomedical diagnosis [3] and health sensor [4] in addition to optical communication [5] and night vision [6] applications. In order to have organic materials performing NIR-responsive character, the most feasible way is to utilize fully conjugated donor-acceptor-type polymers as the donors in conjunction with fullerene derivative as acceptor for OPDs. For example, an OPD device employing a benzodithiophene and dithiadiazolo[3,4-f]benzotriazole hybridized conjugated polymer (PTZBTTT-BDT) blended with $PC_{61}BM$ as the active layer contacted with a cross-linkable fluorene-based polymer (PFN-OX) as electron extraction layer delivered an external quantum efficiency (EQE) of 18.2% at 800 nm.[7] The EQE at 800 nm has been improved to ca. 30% by utilizing a polymeric donor PBD(EDOT) composing of thiophene-linked benzodithiophene and diketopyrrolopyrrole and the acceptor $PC_{61}BM$.[8] In addition to polymeric donors, solution-processed OPDs based on small molecule donors also demonstrated good performance, for example, an OPD using a donor–acceptor porphyrin derivative (DHTBTEZP) as donor and $PC_{61}BM$ as acceptor can give an EQE of 23.5% at 800 nm.[9] The detection range can further extend to 850 nm with a EQE of 17.0% by introducing a cyanine dye Cy7-T as the NIR-responsive material together with a photo-polymerized C_{60} as acceptor. Interestingly, this cyanine dye-based OPD performed transparent character.[10] It is obvious that the fully conjugated polymer as well as small-molecule donors can exhibit efficient NIR-absorption, together with good electron-transporting character of $PC_{61}BM$, rendering the resultant OPDs to have good EQEs in NIR region and low dark current for good sensitivity. However, there are some challenging issues on the lifespan of OPDs fabricated with solution process techniques. One feasible solution for providing OPDs with comparable efficiency as those of solution-processed counterparts but performing better lifetime is to use well-established vacuum process compatible to the current OLED display technology. Unfortunately, the small molecule donors simultaneously fulfill the NIR absorption and thermal stability for vacuum deposition are very limited. Among the reported vacuum-processed NIR OPDs, the ones employing lead phthalocyanine (PbPc) as donor

combining pristine C_{60} as acceptor are the most successful cases. Even with vacuum deposition, there are still some rooms for device engineering, for example, a bilayer-type (PbPc/C_{60}) photo-active configuration has been demonstrated to give an EQE of 18.0% at 900 nm.[11] The efficiency can be further improved to 30.2% at 890 nm with planar-mixed bulk heterojunction (BHJ) configuration, where the photo-responsive PbPc(5%):C_{70} blend was sandwiched between a thin layer of PbPc and C_{70} for better exciton generation as well as electron/hole extraction.[12] In addition, the control of the crystallinity of PbPc has been revealed not only to extend the response region to longer wavelengths but also to enhance the EQE up to 31.1% at 970 nm at a reverse bias of -3 V.[13] In spite of the advantage for efficiently catching photons, organic materials typically possess high electron-hole (exciton) binding energies due to low dielectric constants. [14,15] As consequence, for most organic NIR OPDs with high photogeneration yield, the photo-responsive layer is either donor/acceptor bilayer-type or a donor:acceptor (D:A) blend (namely, a BHJ) not only for facilitating the charge carrier generation by virtue of photo-induced charge separation, but also for effective charge transport and collection.[16] Therefore, both the molecular design and device fabrication are crucial for manipulating the intermixed D:A morphologies. One feasible way for reducing the complexity of making efficient OPD is to use "single component" as the active layer. In this regard, there are still limited cases being reported to perform promising efficiency due to the inferior photogeneration yield of photo-active materials. [17,18] Recently, the direct generation of free carriers by photoexcitation has been observed in some phthalocyanine-type molecules such as zinc phthalocyanine (ZnPc), boron subphthalocyanine chloride (SubPc), and boron subnaphthalocyanine chloride (SubNc) through spectroscopic measurements. [19,20,21] The observed direct generation of free carriers in single-component active layers under photoexcitation presents an interesting evidence that these organic molecules possess extremely low electron-hole binding energies even with low-dielectric constants. Fundamentally, this imposes a critical question on the underlying mechanisms that are accountable for the significantly low electron-hole binding energies in these organic materials. Technically, these results trigger a new possibility for exploring phthalocyanine-based materials as a "single-component" active layer to realize efficient OPDs without using BHJ designs.

In this work, for the first time, we demonstrate a high-efficiency NIR OPD by adopting the single-component active layer (phthalocyanine, ClAlPc) with four-fold symmetry of photoinduced charge density through planar cyclic intramolecular donor-acceptor structures. With

photoexcitation at 780 nm, under a forward bias of 3 V, the device delivered an EQE reaching a record-high value of 43% and the photocurrent gain ratio higher than $3x10^5$. The outstanding performance of this single-component-based OPD implies that the ClAlPc thin film exhibits an extremely low electron-hole binding energy. This result stimulated our efforts to explore the underlying mechanisms responsible for such low electron-hole binding energy when the symmetry of photoinduced charge density exists through planar cyclic intramolecular donor-acceptor structures. By using *in-situ* bias-dependent magneto-photocurrent measurement, the observed critical bias required to complete the dissociation of the electron-hole pairs in four-fold symmetric ClAlPc is extremely low (24.8 mV). The same protocol was also employed to examine other phthalocyanine derivatives, namely, three-fold symmetry SubPc and asymmetrical ClAlNPc. The observed critical bias largely increases to 128 mV for SubPc and 525 mV for ClAlNPc. Based on these results, we propose that the arrangement of photo-induced electric dipoles (phenylene$^{\delta+}$-pyrrole$^{\delta-}$) within planar cyclic intramolecular donor-acceptor structures is a crucial parameter to significantly lower electron-hole binding energies in organic materials towards developing high-efficiency NIR OPDs by using single-component active layer design.

Results and discussion

The device architecture of the single-component active layer NIR OPD was configured as ITO/ClAlPc (10 nm)/TAPC (90 nm)/MoO_3 (15nm)/Al (120 nm) (Figure 1a). The ClAlPc thin film functions as an active layer to directly generate free carriers under NIR photoexcitation. The TAPC/MoO_3 acts as the hole transport layers. Under forward bias (> 0 V), we defined the ITO and Al serving as anode and cathode, respectively. Therefore, the holes (electrons) came from ITO (Al) electrode. In this situation, the holes and electrons were blocked at ITO/ClAlPc and TAPC/MoO_3 interfaces, respectively, due to the potential barriers formed between the HOMO level of ITO (4.8 eV) and ClAlPc (5.3 eV), and the LUMO level of TAPC (2.0 eV) and the work function of MoO_3 (6.9 eV), respectively, leading to the ultra-low current density reaching to 1.2 nA cm^{-2} at an operating forward bias of 1.0 V under dark condition (Figure 1b). Under the 2 mW cm^{-2} photoexcitation from a NIR LED peaked at 780 nm, the photocurrent significantly increases, indicating the efficient generation of free charge carriers in the ClAlPc layer in the absence of BHJ structures. Specifically, the photocurrent gain ratio (defined as the photocurrent divided by dark

current [22,23,24]) reaches to $3x10^5$ at driving voltage of 3 V (Figure 1c) while the EQE at 780 nm become 14% (at zero bias) and 43% (at 3 V) (Figure 1d). Figure S1 shows the EQE of the optimized thickness of 10 nm, 20 nm and 30 nm for the ClAlPc single-layer devices. The EQE decreases obviously with increasing the ClAlPc thickness. In addition to the high EQE and photocurrent gain, the detectivity is another important parameter for evaluating the performance of a photodetector. Here, the specific detectivity was expressed as:

$$D^* = \frac{R}{\sqrt{2qJ_d}}$$

where R is responsivity (A W^{-1}), q is an elementary charge (1.6×10^{-19} Coulomb), and J_d is the dark current density (A cm^{-2}). At the operating wavelength of 780 nm and a bias of 3 V, the specific detectivity (D^*) reaches to 5.8×10^{12} Jones based on our single-component active layer design (Figure S2), which is among the highest detectivity as comparing to those of previously reported NIR OPDs prepared by multiple-component active layer architectures. To understand the correlation between the photocurrent and incident light intensity, we analyzed linear dynamic range (LDR) of a commercial standard silicon-based photodetector (Si-PD, Newport 818-UV) to verify our measurement. As shown in Figure 2a, the LDR of Si-PD under a bias of -0.5 V is as high as 230.6 dB with 11-order magnitude difference of photocurrent response to light power density from 3.78 pW cm^{-2} to 1 W cm^{-2}. For our single-component ClAlPc based OPD, under a bias of 0.5 V, the photocurrent linearly increases from 0.521 nA cm^{-2} to 0.163 A cm^{-2} corresponding to light power density from 2.93 pW cm^{-2} to 1 W cm^{-2}, leading to an LDR of 170 dB with 8-order magnitude difference in photocurrent response. To our best knowledge, the LDR of our single-component ClAlPc-based OPD is the highest one ever reported in NIR-responsive OPDs and comparable to the LDRs (160~200) reported in perovskite-based photoreactors.[25,26,27,28] It is noteworthy to note that the low dark current is revealed as the major factor responsible for the LDR difference between Si-PD and ClAlPc-based OPD. The defective interfacial contact between ITO and organic thin film is generally believed to lead to the higher leakage current of OPD. [29,30] In addition to LDR, the response speed of an OPD is also a crucial parameter, particularly important for optical communication applications. [31,32,33] Figure 2b shows the photocurrent responses of Si-PD and ClAlPc-based OPD under 10 kHz light pulse (780 nm) with an incident power density of 2 mW cm^{-2}. Accordingly, the rise/fall time can be extracted as 0.75/0.7 μs and 0.57/0.64 μs for the ClAlPc-based OPD and Si-PD, respectively. This result indicates that the

response speed of our ClAlPc-based single-component OPD is comparable with the commercial standard Si-PD under same condition. Meanwhile, the charge-carrier mobility of ClAlPc was analyzed with space charge-limited currents (SCLC) method [34,35] by using a hole-only device configured as ITO/MoO_3 (10 nm)/ClAlPc (100 nm)/MoO_3 (10 nm)/Ag (120 nm). As shown in Figure S3, the hole mobility of ClAlPc with the average value of 8.42×10^{-5} cm^2 V^{-1} s^{-1} was obtained in applied electric fields (800 ~ 1000 V cm^{-1}). Noteworthy, although the charge mobility of ClAlPc is significantly lower (4 ~6 orders of magnitude) than that of p-Si, these two photodetectors still show similar response speeds. This result can be attributed to the direct generation of free carriers in the single-active layer (ClAlPc) that allows to use ultra-thin (10 nm) device structure. The dynamic response of Si-PD and ClAlPc-based OPD was measured with response frequency from 100 to 1 M Hz under 780 nm light source with an incident power density of 2 mW cm^{-2}. As shown in Figure 2c, the cut-off frequency of ClAlPc-based OPD and Si-PD is 823.8 and 932.3 kHz at -3 dB, respectively, agreeing with the observed results shown in Figure 2b. Moreover, the aging study showed stable light and dark current densities with continuous light exposure (at 2 mW cm^{-2} 780 nm LED) and 3 V bias of the ClAlPc-based OPD, indicating a decent stability for NIR sensing. (Figure S4).

Clearly, the high NIR photosensing capability in ClAlPc-based single-component active layer NIR OPD indicates the photogenerated electron-hole pairs can be efficiently dissociated into free charge carriers even without using any BHJ design. Here, we notice that the ClAlPc molecule is consisted of four planar isoindole rings symmetrically arranged into a planar cyclic structure with one vertical electric dipole ($Cl^{\delta-}$-$Al^{\delta+}$), as shown in Figure 3a. By arranging four isoindole units with four-fold symmetry in a molecular ring, upon photoexcitation, the intramolecular charge transfer can lead to symmetrically arranged photo-induced electrical dipoles (phenylene$^{\delta+}$-pyrrole$^{\delta-}$) within a molecular ring. Due to the molecular symmetry, these four electrical dipoles (phenylene$^{\delta+}$-pyrrole$^{\delta-}$) encounter symmetrical head-to-head repulsive interactions, consequently decreasing the Coulomb attraction within each electrical dipole. Essentially, this can significantly lower the electron-hole binding energy of ClAlPc. This presents a fundamental principle that introducing the symmetry of photoinduced charge density leads to a large reduction on electron-hole binding energy in organic molecules, known as low-dielectric materials. Here, we directly monitor the dissociation of electron-hole pairs in ClAlPc thin film by using bias-dependent magneto-photocurrent. Generally, the presence of magneto-photocurrent in organic

semiconductors indicates that the electron-hole pairs are formed with singlet and triplet states under photoexcitation for the generation of photocurrent.[36] A magnetic field can change the populations on singlet and triplet electron-hole pairs by perturbing intersystem crossing, leading to the change on photocurrent, generating a magneto-photocurrent, due to the different dissociation rates associated with singlets and triplets.[37] On the other hand, applying an external bias can increase the dissociation of electron-hole pairs, [38,39] decreasing magneto-photocurrent signal. When an external bias reaches a critical value, magneto-photocurrent signal can be completely quenched. Essentially, this critical bias, required to completely quench magneto-photocurrent signal, reflects the electron-hole binding energy. Therefore, combining magneto-photocurrent with external bias provides the convenient experimental tool to *in situ* monitor the dissociation of electron-hole pairs in organic materials when an external bias is applied.[40,41] Figure 3b shows the bias-dependent magneto-photocurrent signal in ClAlPc single-layer device with the structure of ITO/ClAlPc(50 nm)/Al. We can see that the photocurrent gradually increases and then becomes saturated with increasing magnetic field, leading to a magneto-photocurrent signal. More importantly, the magnitude of magneto-photocurrent signal is gradually decreased with increasing bias. This indicates that magneto-photocurrent can indeed reflect the dissociation of electron-hole pairs generated in the ClAlPc film with gradually increasing bias imposed on the ITO/ClAlPc/Al device. By plotting magneto-photocurrent amplitude against bias (Figure 3c), we can determine that the electron-hole pairs are completely dissociated at the low bias of 24.8 mV, indicating the extremely small binding energy of electron-hole pairs, responsible for the efficient free charge carrier generation in ClAlPc molecule. This experimental result brings about a critical question on why free photogenerated carriers can be directly generated in organic materials which normally possess high electron-hole binding energies due to low-dielectric constants.

To verify the symmetry-dependent electron-hole binding energies, we selected organic molecules (SubPc and ClAlNPc) with reduced symmetry of charge density. It is noticed that SubPc have been reported to exhibit direct free charge carrier generation under photoexcitation with notable power conversion efficiency (PCE) of 0.3% in a single-layer device (ITO/SubPc/Al).[20] The SubPc consists of three pyrrole-phenylene (isoindole) moieties with a permanent electric dipole of B^{+}-Cl^{-} (Figure 3d). Clearly, the SubPc molecule possess the three-fold symmetrical arrangement of electrical dipoles (phenylene$^{\delta+}$-pyrrole$^{\delta-}$), leading to three-fold symmetry of charge density. This three-fold symmetric SubPc should exhibit a weaker mutually repulsive interaction

as compared with four-fold symmetry ClAlPc molecule. Indeed, the critical bias required to completely dissociate electron-hole pairs of the SubPc thin film was determined by bias-dependent magneto-photocurrent to be 128 mV, indicating a larger binding energy as compared to that of ClAlPc film (Figure 3 e and f). To further investigate our hypothesis, we employed the same protocol on an asymmetric planar macrocyclic molecule ClAlNPc (Figure 3g) having a structure fused with three pyrrole-phenylene (isoindole) moieties and one pyrrole-naphthylene structure (benzoisoindole). By breaking the symmetry of charge density, the dissociation of electron-hole pairs can become much more difficult, shown as a much higher bias to quench the magneto-photocurrent as indicated by Figure 3h. Thus, completely quenching the magneto-photocurrent requires the bias as high as 525 mV in the device with ClAlNPc thin film, where the symmetry of charge density is removed, as shown in Figure 3i. This result indicates that perturbing the symmetry of charge density in a planar macrocyclic system causes a large increase on electron-hole binding energy. Clearly, increasing the symmetry of charge density presents an important mechanism to lower the electron-hole binding energy in organic macrocyclic molecules typically known as low-dielectric materials. Especially, the extremely low binding-energy in four-fold symmetric ClAlPc molecule significantly facilitates the photogeneration of free carriers in a photodetector with the single-component active layer for realizing the extraordinary NIR photosensing capability. To further explore the application of ClAlPc thin film as a single-component active layer, an ultimate solar cell configured as a single-layer device (ITO/ClAlPc/Al) was examined. This simple device can demonstrate a record-high PCE up to 0.45% with Voc of 0.76 V and Jsc of 1.3 mA cm^{-2} due to the extremely low binding-energy (Figure S5 and Table S1), as compared with all other single-layer organic solar cells.[20] Here, we should point out that molecular packing is not an underlying factor in determining the electron-hole binding energy in ClAlPc films based on following two experimental indications. First, our magneto-photocurrent that was used to determine the electron-hole binding energy is a common phenomenon resulting from intramolecular electron-donating and electron-accepting structures. Second, our grazing-incidence wide-angle X-ray scattering (GIWAXS) and grazing-incidence small-angle X-ray scattering (GISAXS) studies have shown that the ClAlPc films contain crystalline nanograins and amorphous parts, as indicated in supporting information (Section IV). More importantly, such amorphous regions in the vertical direction increase with increasing film thickness (eg. 50 nm) where the record-high PCE was realized in single-layer ClAlPc device configured as

ITO/ClAlPc(50 nm)/Al. Clearly, our bias-dependent magneto-photocurrent measurements provide the direct evidence that that indicates the electron-hole binding energy is significantly lowered by increasing the symmetry of optically generated electrical dipoles within planar macromolecular structures. Overall, these results provide the precondition to further advance organic optoelectronics with a single-component active layer design.

Now we discuss the underlying mechanism responsible for the extremely low electron-hole binding energy. The ClAlPc molecule consists of four symmetrically arranged isoindole rings linked by four nitrogen bridges into a fully conjugated symmetric planar molecular ring with a vertical electric dipole ($Cl^{\delta-}$-$Al^{\delta+}$). Figure 4 shows the electrostatic potential analysis of ClAlPc in excited states. It clearly indicates the charge density is symmetrically distributed on macrocycle. We should note that photoinduced charge transfer occurring at the isoindole moiety from the outer phenylene to inner pyrrole leads to optically generated electric dipoles ($phenylene^{\delta+}$-$pyrrole^{\delta-}$). With the four-fold symmetry of charge density, the four optically generated electric dipoles are symmetrically arranged with head-to-head configuration. Essentially, these symmetrically arranged optically generated electric dipoles with head-to-head configuration can decrease the attractive interaction between $phenylene^{\delta+}$ and $pyrrole^{\delta-}$ within each dipole, serving as the requirement to significantly lower the binding energy of photogenerated electron-hole pairs towards direct generation of photogenerated carriers. We should point out that this vertical dipole ($Cl^{\delta-}$-$Al^{\delta+}$) can significantly stabilize the formation of optically generated dipoles ($phenylene^{\delta+}$-$pyrrole^{\delta-}$) with four-fold symmetry in ClAlPc molecules. Without this vertical dipole, optically excited electrons in the inner ring have the possibilities to quickly relax back to the outer ring. Therefore, it is essential that the lifetime of optically generated dipoles must be sufficiently longer than the dissociation time of electron-hole pairs to demonstrate significantly reduced electron-hole binding energy. To verify our scenario, the parent phthalocyanine (Pc) without the electric dipoles ($phenylene^{\delta+}$-$pyrrole^{\delta-}$) was investigated (Figure S6a). The absorption coefficient of Pc is similar to those of ClAlNPc and ClAlPc molecules. It is interesting to note that it requires an extremely large bias up to 2.35 V to completely quench magneto-photocurrent signal (Figure S6b and c), indicating high electron-hole binding energy in Pc molecule. In addition, the corresponding single layer-based device (ITO/Pc/Al) delivered a negligible photovoltaic effect with a PCE less than 0.01% (Figure S6d). Clearly, the vertical electric dipole plays an important role to realize the low binding energy through head-to-head interaction under symmetric charge density.

To verify the formation of optically generated electrical dipoles through photoinduced charge transfer, the capacitance-frequency characteristics were examined for the ClAlPc at different photoexcitation intensities (Figure 5a). We can see that the photoexcitation clearly increases the signal amplitude around 1 kHz on capacitance-frequency (C-f) characteristics in the ClAlPc molecule while the ClAlNPc molecule shows a negligible change upon applying photoexcitation (Figure 5b). The photoexcitation-dependent C-f characteristics provide an evidence to support that the electron withdrawing (pyrrole) and donating (phenylene) units respectively become negatively and positively charged within the ClAlPc molecule as the consequence of exciton dissociation due to extremely low electron-hole binding energy. In contrast, the photoinduced C-f curve (Figure S6e) of the Pc molecule shows an obvious enhancement at low frequency (less than 1 k Hz), indicating the surface charge accumulation due to the insufficient charge transport without permanent dipole ($Cl^{\delta-}$-$Al^{\delta+}$). As comparison, the ClAlNPc molecule with asymmetric planar molecular cyclic structure does not demonstrate appreciable photoexcitation-dependent C-f characteristics, confirming the absence of dissociated charge carriers due to the high electron-hole binding energy.

Conclusions

In summary, we have demonstrated the high NIR sensing capability with the photocurrent gain of $3x10^5$, and the EQE of 14 % (at zero bias) and 43 % (at 3V) by using the four-fold symmetric ClAlPc molecules as the single-active layer without BHJ structures. Moreover, this single component (ClAlPc) active layer OPD exhibits record-high linear dynamic range (LDR) of 170 dB with 8-order magnitude difference in photocurrent response and sub-microsecond response time, comparable with the commercial Si-PD. The extraordinary performance of ClAlPc-based OPD device indicates that the electron-hole binding energy must be surprisingly low to effectively dissociate photogenerated electron-hole pairs towards direct generation of free carriers under photoexcitation. More importantly, our bias-dependent magneto-photocurrent studies found that introducing the symmetry of charge density with planar molecular ring provides a fundamental mechanism to significantly lower the electron-hole binding energy in organic molecules known as low-dielectric materials. We observed that the critical bias required to complete the dissociation of photogenerated electron-hole pairs reaches an extremely low value of 24.8 mV in four-fold

symmetry ClAlPc molecules. This reflects a significantly reduced electron-hole binding energy when introducing the four-fold symmetry of charge density through molecular design of planar macrocyclic conjugated ring systems. Furthermore, the vertical electric dipole ($Cl^{\delta-}$-$Al^{\delta+}$) can facilitate electron-hole pairs dissociation and electrical conduction in four-fold symmetry ClAlPc molecules. In contrast, decreasing the symmetry of charge density to three-fold structure, the SubPc molecules demonstrate a higher critical bias of 128 mV to complete the dissociation of electron-hole pairs. Furthermore, by breaking the symmetry of charge density, the critical bias required to dissociate the electron-hole pairs is largely increased to 525 mV in the analogous counterpart ClAlNPc with asymmetric molecular ring composing of three planar isoindole rings and one benzoisoindole ring. Clearly, increasing the symmetry of charge density can lead to an extraordinary NIR photosensing capability by using the ClAlPc molecules as single-component active layer based on the device architecture of ITO/ClAlPc (10 nm)/TAPC (90 nm)/MoO_3 (15 nm)/Al (120 nm). Fundamentally, our bias-dependent magneto-photocurrent studies indicate that increasing the symmetry of charge density presents an underlying mechanism to significantly lower the electron-hole binding energies in organic molecules for energy related optoelectronic applications.

Experimental Methods

Materials and Devices Fabrication: The chloroaluminum phthalocyanine (ClAlPc), phthalocyanine (Pc), boron subphthalocyanine chloride (SubPc) 1,1-bis(di-4-tolylaminophenyl) cyclohexane (TAPC), MoO_3 and Al, were purchased from Sigma Aldrich. The asymmetrical ClAlNPc was synthesized by us and the detailed synthesis procedure can be found in the supporting information. The organic material of ClAlPc was sublimated twice by using a homemade purification system according to previously reported procedures. The ITO substrates with a sheet resistance of approximately 15 ohm sq^{-1} were purchased from Luminescence Technology Corporation. For the cleaning process, the sample was cleaned in an ultrasonic bath in successive solutions, dilute detergent, acetone, and isopropanol, and soaked in a DI water. Organic thin-film was deposited by using a thermal evaporator with a high vacuum of 5×10^{-6} Torr, while the quartz crystal monitor was detected the film thickness in situ. Note that all fabrication processes were appropriately encapsulated in a nitrogen-filled glove box. For

measurement, our device's active area of 4 mm^2 was defined by cross-area of anode and cathode pads.

Theoretical Calculation: The calculations were accomplished with Guassian 09 suit of programs through Taiwania. The ground state geometry optimizations of **ClAlPc** and **ClAlNPc** were conducted in gaseous state at a B3LYP/6-31g(d,p) level via utilizing density functional theory (DFT). The S_1 state geometry optimizations of **ClAlPc** and **ClAlNPc** were conducted in gaseous state at a B3LYP/6-31g(d,p) level via utilizing time-dependent density functional theory (TD-DFT). All the electrostatic potential surface (ESP) were attained after the geometry optimization and mapped at the 0.047 electron density. We are grateful to the National Center for High-performance Computing for computer time and facilities for the computing resources.

Measurements and Characterizations: In the photodetector performance characterizations, the current density-voltage characteristics of NIR OPDs were measured with a source meter (Keithley 2636A) in the dark and under a 780 nm illumination (Thorlabs LED780L) at 2 mW cm^{-2}, respectively. The device's current gain ratio was defined as the light current density divided by dark current density. To performance the photovoltaics characteristics for single active layer devices (ITO/active layer/Al), the devices were measured with a current source meter (Keithley 2401) under dark and under AM 1.5G solar simulator (Newport 91160). Note that the intensity of 1 sun (100 mW cm^{-2}) was calibrated by through a Si reference cell (PV Measurement; area: 3.981 cm^2). A monochromator (Newport 74100) and lock-in amplifier (Signal Recovery 7265) chopped at 250 Hz were used to evaluate the EQE of our devices. The absorption spectrum of the organic layer was determined using an ultraviolet (UV)-visible spectrophotometer (Thermo Scientific Evolution 220). For linear dynamic range (LDR) measurement, the illumination source was used the NIR LED (Thorlabs LED780L) and laser Model (CNI MLL-III-785) to irradiate the OPDs, while the device's photocurrent was recorded using a source meter (Keithley 2636). To adjust the pumping intensity, the optical wheel with ND filter can turn to set the various power density from 1 W cm^{-2} to 10 pW cm^{-2}, which calibrated by the precision power meter (Newport power meter Model 1936-R). To estimate the LDR value, we used the equation LDR (dB)=$20\log(J_{ph}/J_{dark})$, where J_{ph} and J_{dark} represent the photocurrent of the device obtained under a light (1 W cm^{-2}) and dark (10 pW cm^{-2}) conditions. For the photocurrent response behavior measurement, the LED (Thorlabs LED780L) with a pulse width of 10 kHz was modulated by the function generator

(Tektronix AFG3120C) as excitation NIR light source (780 nm). The light intensity was set at 2 mW cm^{-2}. Our proposed photodiode was connected to the 2.5 GHz oscilloscope (LeCroy Waverunner 625Zi) with pre-amplifier (Signal Recovery 5182 Model). The frequency response was recorded with a NIR LED (Thorlabs LED780L) driven by a function generator (Tektronix AFG3120C) to create a pulse waveform with a frequency from 10^2 to 10^6 Hz. The measurement signal was used the pre-amplifier (Signal Recovery 5182 Model) to connect a digital oscilloscope (LeCroy Waverunner 625Zi). Then, the raw data were analyzed using the Fast Fourier Transformation to calculate the value of cut-off frequency. The stability test was performed in encapsulated devices at ambient condition with the temperature of 27 °C and the humidity of 60%. The magneto-photocurrent signals were measured by monitoring the photocurrent value (Keithley 2400) as a function of magnetic field at room temperature. The magneto-photocurrent amplitude is defined as: $MFE = \frac{I_B - I_0}{I_0}$, where I_B and I_0 are the photocurrents with and without an external magnetic field. The photoexcitation was from 785 nm CW laser. The impedance measurements were carried out by using Agilent E4980A LCR meter under an alternating bias of 50 mV.

Conflicts of interest

There are no conflicts to declare.

Author contributions

M. W. performed the bias-dependent magneto-photocurrent measurements and C-f measurements. B. H. supervises the experimental studies. Y. -Z. L., and C. -W. L., prepared and characterized the OPDs, the hole-only devices for the SCLC and the OPVs. H.-C. C. synthesized and characterized ClAlNPc molecule. Y. -S. C. and Y. -C. L. conducted the theoretical analyses of excited state electrostatic potential maps. C. -S. T. and Y. -C. H. conducted the GIWAXS and GISAXS analyses. M. W., S. -W. L., K. -T. W. and B. H. provide ideas for rationalizing the results and prepare the manuscript.

Acknowledgements

This research was supported by the financial supports from Air Force Office of Scientific Research (AFOSR) under the grant number FA 9550-15-1-0064, AOARD (FA2386-15-1-4104), and National Science Foundation (NSF-1911659). This research was partially conducted at the Center for Nanophase Materials Sciences based on user projects (CNMS2017-102), which is sponsored by Oak Ridge National Laboratory by the Division of Scientific User Facilities, U.S. Department of Energy. The supports granted from the Ministry of Science and Technology Taiwan (107-2113-M-002-019-MY3, 107-2119-M-131-001, 108-2221-E-131-027-MY2) are also acknowledged.

Figures

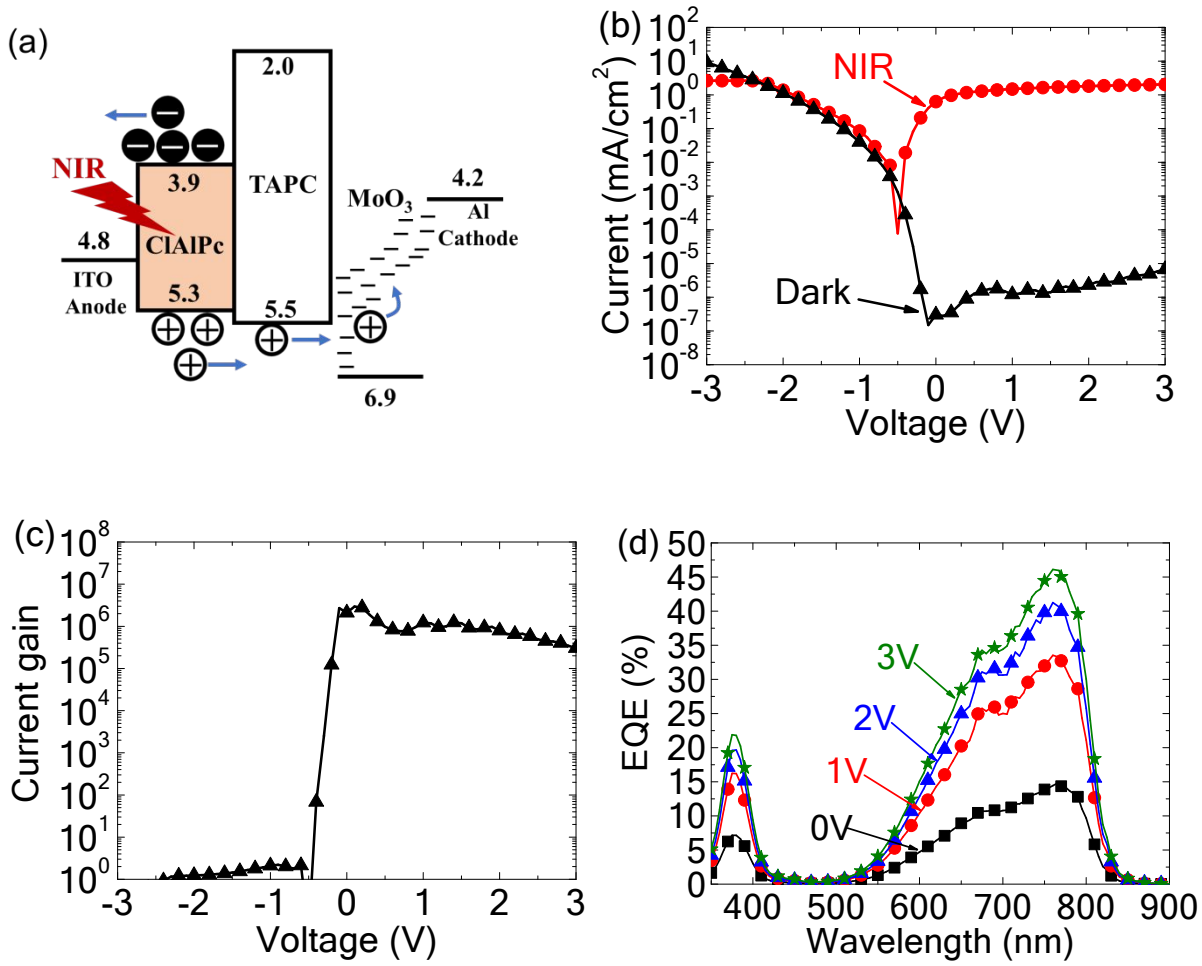

Figure 1. Photodetector device performance characterization. (a) Energy-level diagram for photodetector with ClAlPc as charge generation layer. The device structure is ITO/ClAlPc (10 nm)/TAPC (90 nm)/MoO_3 (15 nm)/Al (120 nm). (b) I-V curves under dark condition and NIR condition for ClAlPc based photodetector. The NIR photoexcitation was provided by a 780 nm NIR LED with the intensity of 2 mW cm^{-2}. (c) Current gain, defined as the photocurrent divided by dark current, is shown as function of bias. (d) EQE spectra under various biases.

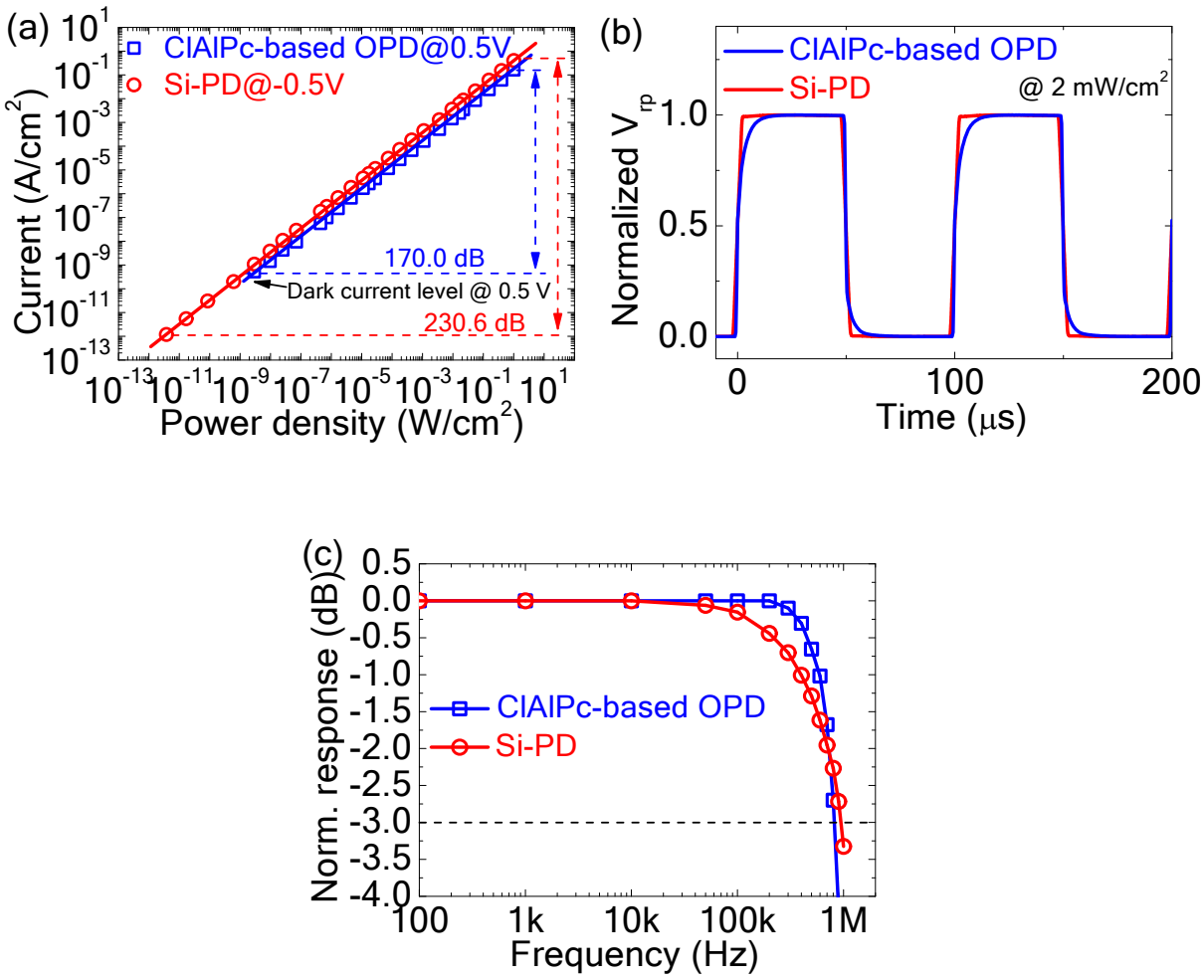

Figure 2. (a) The comparison on linear dynamic range (LDR) for the ClAlPc-based OPD and commercial Si-PD (Newport 818-UV photodetector). The solid lines are the linear fitting. (b) Photocurrent response of ClAlPc-based OPD and the standard Silicon PD to a 10 kHz light pulse at 780 nm with an incident power density of 2 mW cm^{-2}. (c) The cut-off frequency (f_{-3dB}) in Hz at reverse bias (3 V for ClAlPc-based OPD; -1 V for Si-PD).

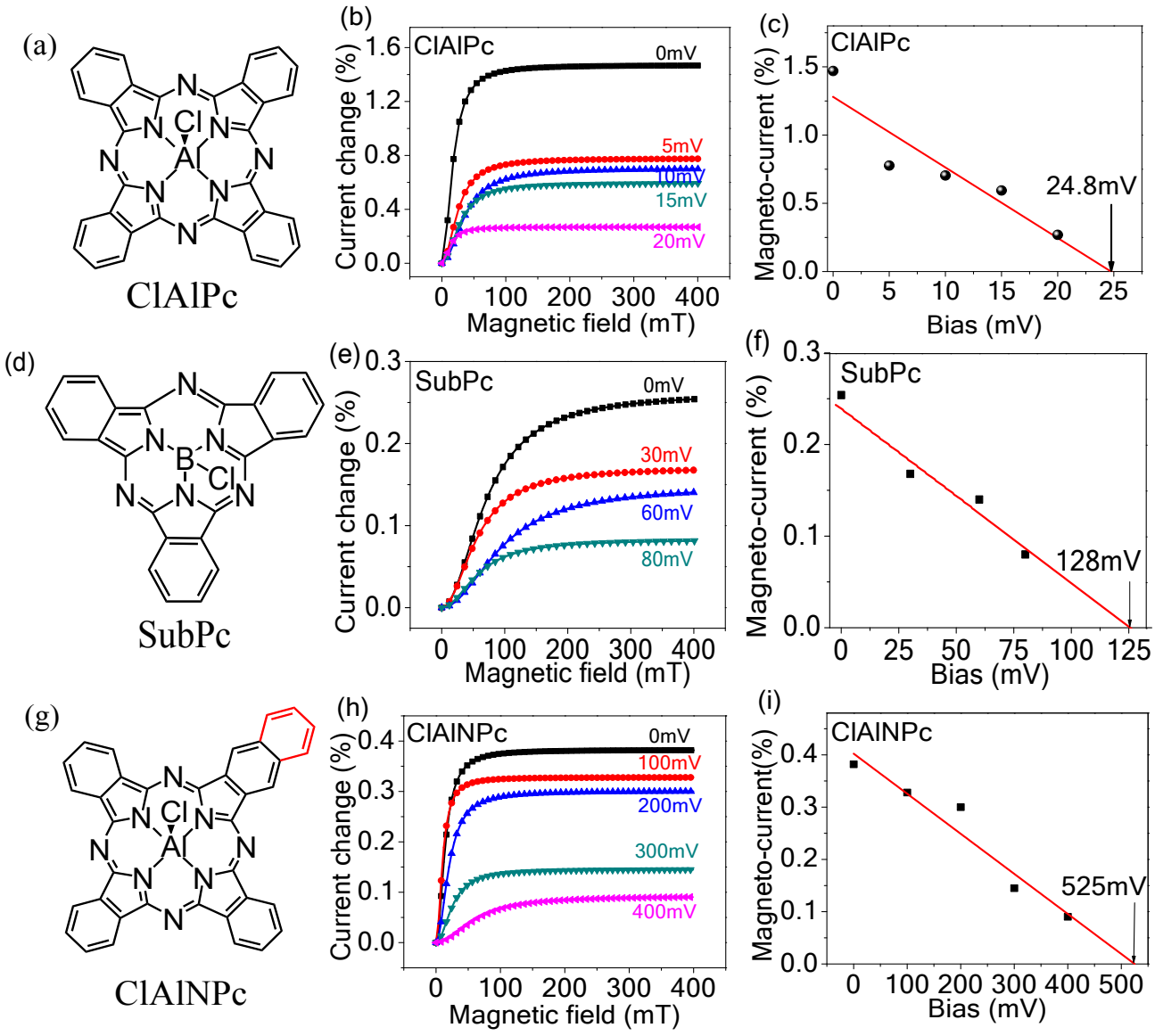

Figure 3. Bias-dependent magneto-photocurrent for ClAlPc and ClAlNPc. (a) Chemical structures for ClAlPc molecule. (b) bias dependent magneto-photocurrent and (c) magneto-photocurrent as the function of applied reverse bias for single layer ClAlPc device (ITO/ClAlPc 50nm/Al). (d) Chemical structure of SubPc molecule. (e) bias-dependent magneto-photocurrent and (f) maximum magnitude of magneto-photocurrent as the function of applied reverse bias for single-layer device (ITO/SubPc (50 nm)/Al). (g) Chemical structure of ClAlNPc molecule. (h) bias dependent magneto-photocurrent and (i) magneto-photocurrent as the function of applied reverse bias for single-layer ClAlNPc device (ITO/ClAlNPc (50 nm)/Al).

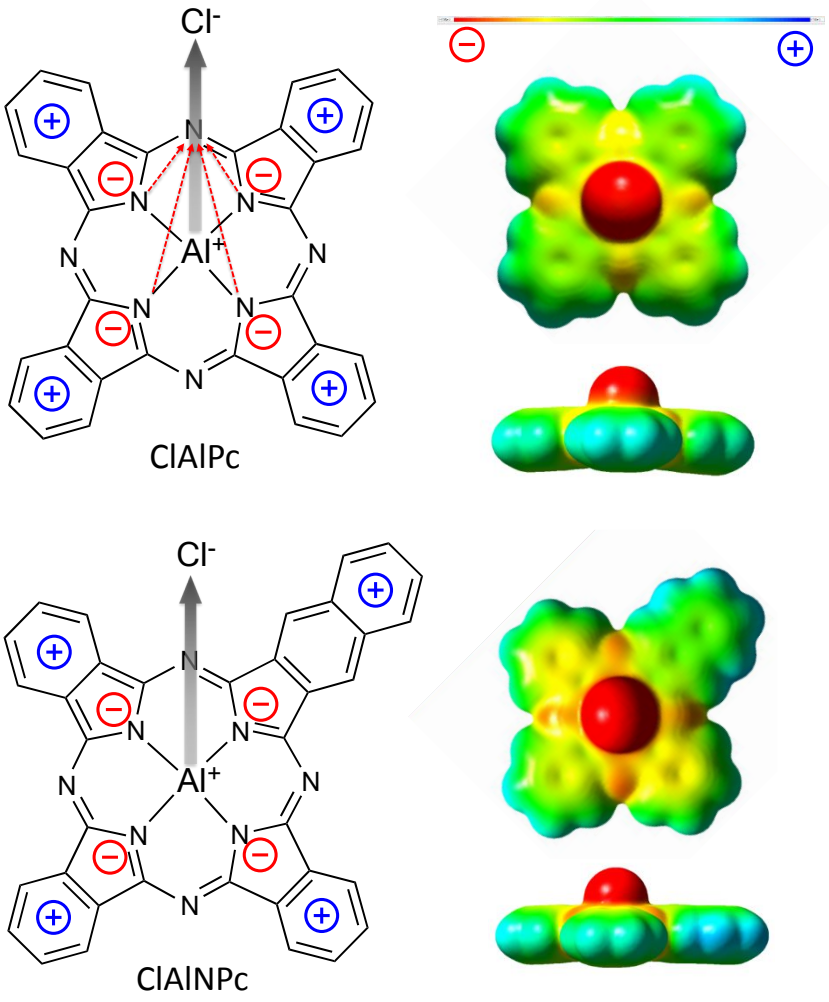

Figure 4. Symmetrically arranging four isoindole rings of ClAlPc with a vertical electric dipole ($Cl^{\delta-}$-$Al^{\delta+}$) and asymmetrically arranging three isoindole rings and one benzoisoindole of ClAlNPc structure with a vertical electric dipole ($Cl^{\delta-}$-$Al^{\delta+}$) and the calculated excited state electrostatic potential maps of ClAlPc and ClAlNPc.

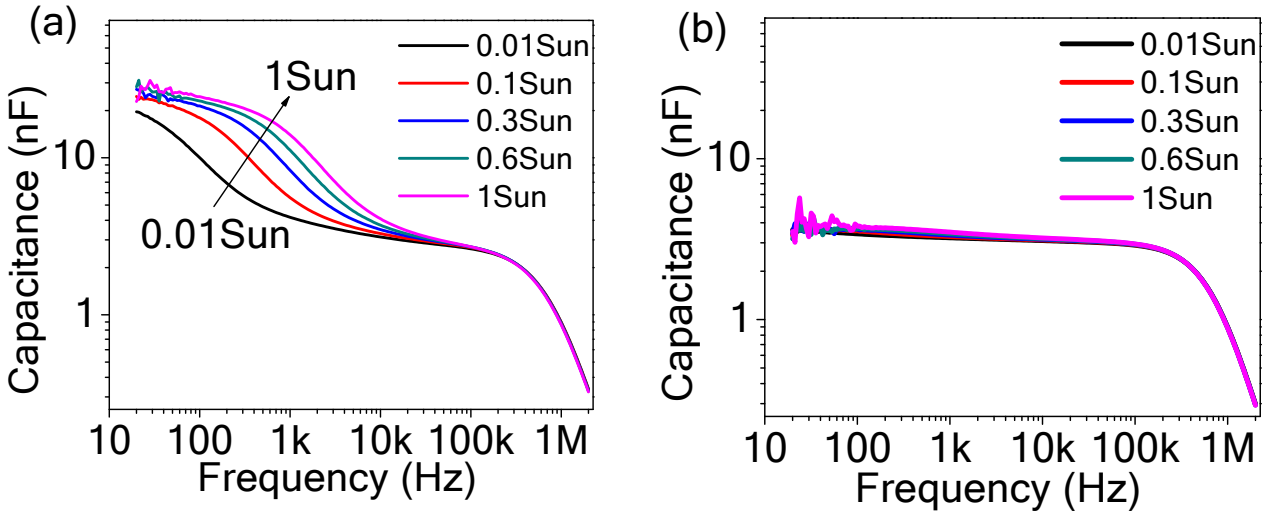

Figure 5. C-f curves under simulated sunlight with variable intensities. (a) ClAlPc device (ITO/ClAlPc (50 nm)/Al). (b) ClAlNPc device (ITO/ClAlNPc (50 nm)/Al).

Reference

[1] H. Tanaka, T. Yasuda, K. Fujita and T. Tsutsui, *Adv. Mater.*, 2006, **18**, 2230-2233.

[2] G. Simone, D. Di Carlo Rasi, X. de Vries, G. H. Heintges, S. C. Meskers, R. A. Janssen and G. H. Gelinck, *Adv. Mater.*, 2018, **30**, 1804678.

[3] Z. Wu, Y. Zhai, W. Yao, N. Eedugurala, S. Zhang, L. Huang, X. Gu, J. D. Azoulay and T. N. Ng, *Adv. Funct. Mater.*, 2018, **28**, 1805738.

[4] S. Park, K. Fukuda, M. Wang, C. Lee, T. Yokota, H. Jin, H. Jinno, H. Kimura, P. Zalar and N. Matsuhisa, *Adv. Mater.*, 2018, **30**, 1802359.

[5] J. Clark and G. Lanzani, *Nat. Photonics*, 2010, **4**, 438.

[6] E. H. Sargent, *Adv. Mater.*, 2008, **20**, 3958-3964.

[7] X. Hu, K. Wang, C. Liu, T. Meng, Y. Dong, S. Liu, F. Huang, X. Gong and Y. Cao, *J. Mater. Chem. C*, 2014, **2**, 9592-9598.

[8] L. Zhang, T. Yang, L. Shen, Y. Fang, L. Dang, N. Zhou, X. Guo, Z. Hong, Y. Yang and H. Wu, *Adv. Mater.*, 2015, **27**, 6496-6503.

[9] L. Li, Y. Huang, J. Peng, Y. Cao and X. Peng, *J. Mater. Chem. C*, 2014, **2**, 1372-1375.

[10] H. Zhang, S. Jenatsch, J. De Jonghe, F. Nüesch, R. Steim, A. C. Véron and R. Hany, *Sci. Rep.*, 2015, **5**, 9439.

[11] X. Wang, H. Li, Z. Su, F. Fang, G. Zhang, J. Wang, B. Chu, X. Fang, Z. Wei and B. Li, *Org. Electron.*, 2014, **15**, 2367-2371.

[12] Z. Su, F. Hou, X. Wang, Y. Gao, F. Jin, G. Zhang, Y. Li, L. Zhang, B. Chu and W. Li, *ACS Appl. Mater. Interfaces*, 2015, **7**, 2529-2534.

[13] M.-S. Choi, S. Chae, H. J. Kim and J.-J. Kim, *ACS Appl. Mater. Interfaces*, 2018, **10**, 25614-25620.

[14] S. R. Forrest, *Nature*, 2004, **428**, 911.

[15] M. Knupfer, *Appl. Phys. A*, 2003, **77**, 623-626.

[16] W. Wang, F. Zhang, M. Du, L. Li, M. Zhang, K. Wang, Y. Wang, B. Hu, Y. Fang and J. Huang, *Nano letters*, 2017, **17**, 1995-2002.

[17] R. K. Canjeevaram Balasubramanyam, A. E. Kandjani, C. J. Harrison, S. S. A. Abdul Haroon Rashid, Y. M. Sabri, S. K. Bhargava, R. Narayan, P. Basak and S. J. Ippolito, *ACS Appl. Mater. Interfaces*, 2017, **9**, 27875-27882.

[18] K. Karimov, S. Moiz, M. M. Tahir, N. Ahmed, R. Tariq, S. Abbas and Q. Zafar, *J Optoelectron Adv Mater*, 2014, **16**, 1430-1435.

[19] X. He, G. Zhu, J. Yang, H. Chang, Q. Meng, H. Zhao, X. Zhou, S. Yue, Z. Wang and J. Shi, *Sci. Rep.*, 2015, **5**, 17076.

[20] H. T. Chandran, T. W. Ng, Y. Foo, H. W. Li, J. Qing, X. K. Liu, C. Y. Chan, F. L. Wong, J. A. Zapien and S. W. Tsang, *Adv. Mater.*, 2017, **29**, 1606909.

[21] K. Cnops, B. P. Rand, D. Cheyns, B. Verreet, M. A. Empl and P. Heremans, *Nat. Commun.*, 2014, **5**, 3406.

[22] S. W. Liu, C. C. Lee, C. H. Yuan, W. C. Su, S. Y. Lin, W. C. Chang, B. Y. Huang, C. F. Lin, Y. Z. Lee and T. H. Su, *Adv. Mater.*, 2015, **27**, 1217-1222.

[23] S.-W. Liu, Y.-Z. Li, S.-Y. Lin, Y.-H. Li and C.-C. Lee, *Org. Electron.*, 2016, **30**, 275-280.

[24] C.-H. Yuan, C.-C. Lee, C.-F. Liu, Y.-H. Lin, W.-C. Su, S.-Y. Lin, K.-T. Chen, W.-C. Chang, Y.-Z. Li and T.-H. Su, *Sci. Rep.*, 2016, **6**, 32324.

[25] J. Miao and F. Zhang, *J. Mater. Chem. C*, 2019, **7**, 1741-1791.

[26] W. L. Tsai, C. Y. Chen, Y. T. Wen, L. Yang, Y. L. Cheng and H. W. Lin, *Adv. Mater.*, 2019, **31**, 1900231.

[27] H. L. Zhu, Z. Liang, Z. Huo, W. K. Ng, J. Mao, K. S. Wong, W. J. Yin and W. C. Choy, *Adv. Funct. Mater.*, 2018, **28**, 1706068.

[28] W. Wang, D. Zhao, F. Zhang, L. Li, M. Du, C. Wang, Y. Yu, Q. Huang, M. Zhang and L. Li, *Adv. Funct. Mater.*, 2017, **27**, 1703953.

[29] Y.-H. Tak, K.-B. Kim, H.-G. Park, K.-H. Lee and J.-R. Lee, *Thin Solid Films*, 2002, **411**, 12-16.

[30] F. Nüesch, E. Forsythe, Q. Le, Y. Gao and L. Rothberg, *J. Appl. Phys.*, 2000, **87**, 7973-7980.

[31] D. Yang and D. Ma, *Adv. Opt. Mater.*, 2019, **7**, 1800522.

[32] R. D. Jansen-van Vuuren, A. Armin, A. K. Pandey, P. L. Burn and P. Meredith, *Adv. Mater.*, 2016, **28**, 4766-4802.

[33] J. Miao and F. Zhang, *Laser Photonics Rev.*, 2019, **13**, 1800204.

[34] P. W. Blom, M. De Jong and J. Vleggaar, *Appl. Phys. Lett.*, 1996, **68**, 3308-3310.

[35] C.-F. Lin, S.-W. Liu, C.-C. Lee, J.-C. Hunag, W.-C. Su, T.-L. Chiu, C.-T. Chen and J.-H. Lee, *Sol. Energy Mater. Sol. Cells*, 2012, **103**, 69-75.

[36] Z. Xu and B. Hu, *Adv. Funct. Mater.*, 2008, **18**, 2611-2617.

[37] A. Schellekens, W. Wagemans, S. Kersten, P. Bobbert and B. Koopmans, *Phys. Rev. B*, 2011, **84**, 075204.

[38] V. Mihailetchi, L. Koster, J. Hummelen and P. Blom, *Phys. Rev. Lett.*, 2004, **93**, 216601.

[39] D. Veldman, O. Ipek, S. C. Meskers, J. r. Sweelssen, M. M. Koetse, S. C. Veenstra, J. M. Kroon, S. S. van Bavel, J. Loos and R. A. Janssen, *J. Am. Chem. Soc.*, 2008, **130**, 7721-7735.

[40] Y.-C. Hsiao, T. Wu, M. Li, W. Qin, L. Yu and B. Hu, *Nano Energy*, 2016, **26**, 595-602.

[41] H. Xu, M. Wang, Z.-G. Yu, K. Wang and B. Hu, *Adv. Phys.*, 2019, **68**, 49-121.

ToC

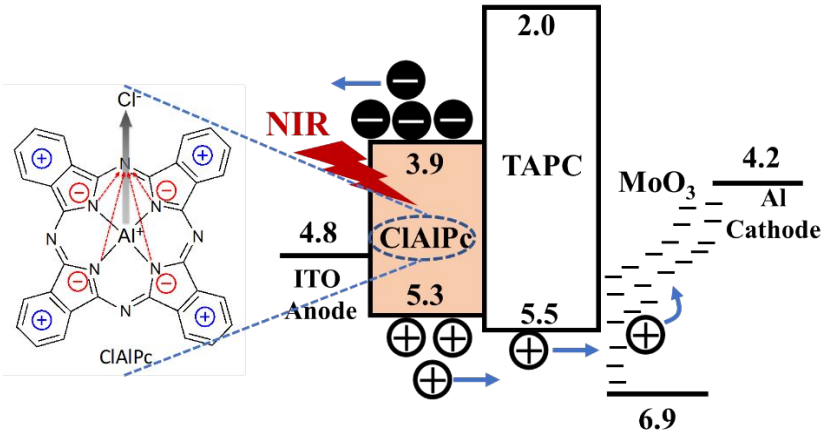

The record-high efficiency single active layer organic near-infrared photodetector is demonstrated with the directly generated free photocarriers.